BMZ-0.9-RHA, BMZ-1.5-RHA corresponding to 0.3g, 0.9g, and 1.5g of CTAB per 100 mL of the aluminosilicate solution, respectively.

Characterization

The samples in this study have been characterized by several techniques to determine the structural properties, the morphology, the specific surface area, and the pore-size distribution. The crystal structure of the catalysts was analyzed by X-ray diffraction (XRD, D8 diffraction) using Cu Kα radiation (= 1.5418Å) operating at 40 kV and 30 mA. Surface morphology of samples observed by scanning electron microscopy (SEM, JEOL - JSM 5500) operating at 10 kV. The specific surface area of the samples was determined from the adsorption of N2 at 77K using the NOVA 2200e equipment (Quantachrome Coop.). The surface areas were obtained from the N2 adsorption using the Brunauer–Emmett–Teller (BET) theory. Moreover, to clarify the mesoporous structure of the materials, the pore size distribution has been also examined. For this measurement, the samples were firstly pretreated at 300°C for 5 hours under a high vacuum condition (P < 0.01 mmHg). After that, the samples were subjected to N_2 adsorption at 77K using liquid nitrogen as a coolant media. The N_2 adsorption was measured in the pressure range P/P_o= 0.03 – 0.99. After that, the N_2 desorption step was also conducted at the same temperature to determine the hysteric behaviors of the material surface to the N_2 adsorption-desorption process. The BJH method (Barrett, Joyner, and Halenda) was then applied for calculating pore size distributions from experimental isotherms using the Kelvin model of pore filling.

Results and discussion

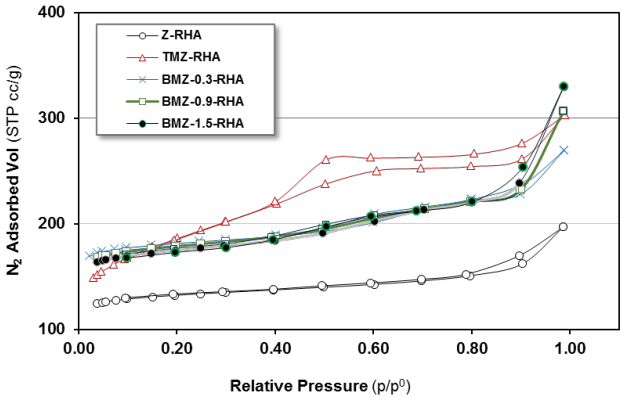

Figure 1: Sorption isotherm for Z-RHA and TMZ-RHA, and BMZ-RHA

Figure 1 demonstrated the adsorption-desorption curves of the rice-husk-ash derived zeolite, the Z-RHA sample, the top-down synthesized mesoporous zeolite TMZ-RHA, and the bottom-up synthesized mesoporous zeolite BMZ-RHA. It can be seen that, in the case of the Z-RHA sample, the adsorption curve and the desorption curve were almost coincidental. Additonally, the fact that there was no hysteresis appeared over the Z-RHA indicating the pore of the Z-RHA were only micropores, in which the capillary condensation phenomenon cannot occur. This observation was again confirmed the zeolite structure of the Z-RHA. The FAU zeolite possesses with size ~ 0.74 nm which was in the micropore range of less than 2 nm according to IUPAC. On the other hand, in the case of the top-down (TMZ-RHA) and bottom-up (BMZ-RHA) synthesized mesoporous zeolites, the adsorption/desorption isotherms showed a typical type IV curve as evidence to identify the capillary condensation phenomenon due to the newly emerging mesopore in the material.

Using the Kelvin model of pore filling, the BJH method (Barrett, Joyner, and Halenda) was then applied for calculating pore size distributions from experimental isotherms in Figure 1. As shown in Figure 2, the contribution of mesopores in Z-RHA (2 nm – 50 nm) to the pore volume was insignificant. On the other hand, in the case of the top-down synthesized mesoporous zeolite TMZ-RHA as well as the bottom-up synthesized mesoporous zeolite BMZ-RHA, it is seen that mesopores were generated in the material structure and these pores were 30-60 A (3-6 nm).

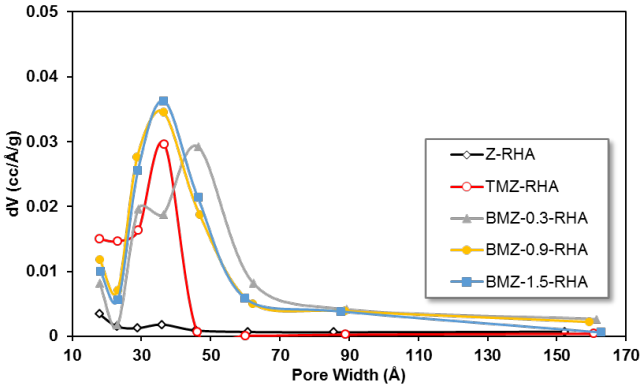

Figure 2: Pore size distribution of Z-RHA and TMZ-RHA and BMZ-RHA

Table 1 summarized the changes in specific surface areas as well as the pore volume when the rice-husk-ash derived zeolite, the Z-RHA sample, has been converted to the mesoporous zeolite (TMZ-RHA) by top-down route as well as bottom-up method. Due to the appearance of more mesopores (3-4 nm) in the material, the mesopore surface area had increased significantly in comparison to the original sample. The

surface area of mesopores in the TMZ-RHA was 151 m^2/g while that of the Z-RHA was 64 m^2/g. Thus, the surface area of mesopores in the sample TMZ-RHA was more than twice as that of the sample Z-RHA (the parent zeolite). Similarly, the total pore volume was also increased significantly. The total volume of the TMZ-RHA was 0.47 mL/g while that of the Z-RHA was 0.26 mL/g. It means that the total pore volume of the zeolite has been increased by about 60% after the top-down modification step. Additionally, as can see from Table 1, the increase of mesopore volume in the mesoporous zeolite was the main contribution to the increase of the total pore volume. Therefore, with the results obtained above and the results of XRD analysis, it can be concluded that mesoporous zeolite had been successfully prepared by the top-down method.

In comparison, BMZ-RHA samples which were prepared by bottom-up approach, as shown in Table 1, have smaller mesoporous surface area than the sample TMZ-RHA. Increasing the amount of added CTAB from 0.3g/100mL to 1.5g/100mL led to the increase of mesoporous surface area and mesoporous volume of the BMZ-RHA. The mesopore surface area was increased from 85 m^2/g to 123 m^2/g while the mesoporous volume was raised from 0.173 mL/g to 0.295 mL/g.

Figure 3 reported results from X-ray Powder Diffraction (XRD) analysis of the rice husk ash (RHA), the rice-husk-ash derived zeolite (Z-RHA), and the mesoporous zeolite prepared by top-down method (TMZ-RHA). As reflected in Figure 3, a SiO_2 crystalline peak has appeared in the case of the RHA at the 2θ ~ 23° which was possibly due to the crystalline surface in RHA generated after high-temperature combustion. The characteristic diffraction peaks of zeolite structure in Z-RHA and TMZ-RHA could be observed at 2θ ranging from 0 to 20°. Basing on the standard XRD pattern, it was confirmed that NaX zeolite within all peaks of Faujasite ($Na_2Al_2Si_{2.4}O_{8.8}.6.7H_2O$, PDF#12-0246) has been obtained in the Z-RHA as well as TMZ-RHA. This indicated that the zeolite X structure was formed in both pre- and post-modified material and the modification process did not alter the crystal structure. However, the intensity and sharpness of the diffraction peaks of the TMZ-RHA sample in the region 2θ from 20° onward were decreased compared to the Z-RHA sample. This may be due to the dissolution of solid crystals in the zeolite sample during the preparation process to create mesoporous zeolite. Additionally, it was also noted that the FAU structure was observed in the BMZ-RHA samples from XRD analysis (data not shown). Therefore, both top-down and bottom-up method could be used to produce FAU zeolite.

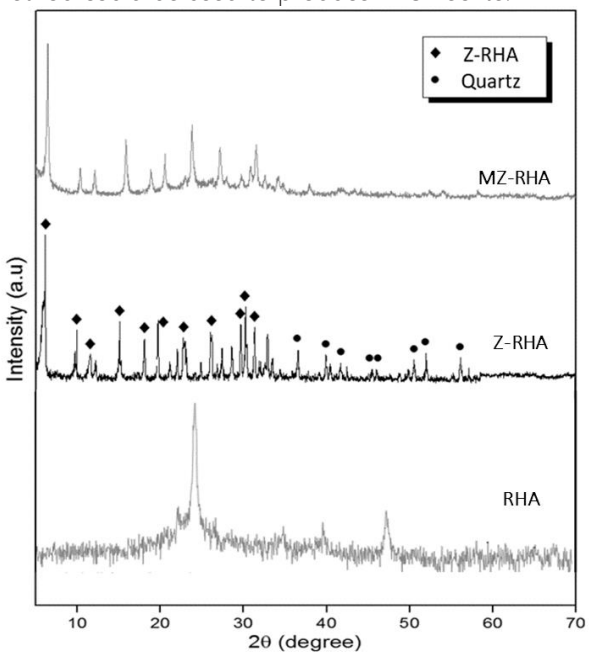

Figure 3: XRD patterns of RHA, Z-RHA and TMZ-RHA.

The morphology of the rice husk ash and the zeolites was also reported. Figure 4 and Figure 5 reported the SEM images of the rice husk ash, the rice-husk-ash derived zeolite, the Z-RHA sample, and the top-down synthesized mesoporous zeolite, sample TMZ-RHA. The size and shape of the rice husk ash were non-uniform while the surface of Z-RHA was smooth and had a uniform size of about 2 - 2.5 μm. The zeolite particles were relatively consistent in shape as well as evenly distributed.

Table 1: Specific surface area and porous properties of Z-RHA, TMZ-RHA, BMZ-RHA

Sample	Specific surface area (m^2/g)	Micropore surface area (m^2/g)	Mesopore surface area (m^2/g)	Micropore volume (mL/g)	Mesopore volume (mL/g)	Total pore volume (mL/g)
Z-RHA	406	341	64	0.175	0.082	0.257
TMZ-RHA	614	463	151	0.123	0.330	0.469
BMZ-0.3-RHA	691	606	85	0.244	0.173	0.417
BMZ-0.9-RHA	670	549	121	0.224	0.252	0.476
BMZ-1.5-RHA	655	532	123	0.217	0.295	0.512

http://doi.org/10.51316/jca.2020.071

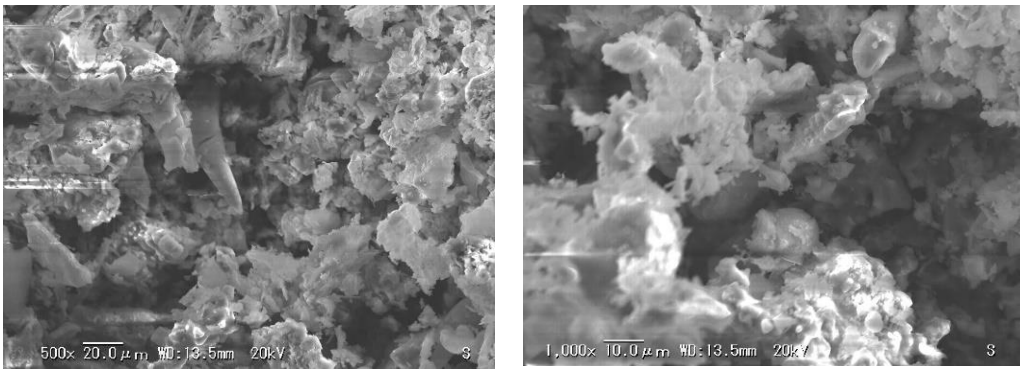

Figure 4: SEM images of the rice husk ash

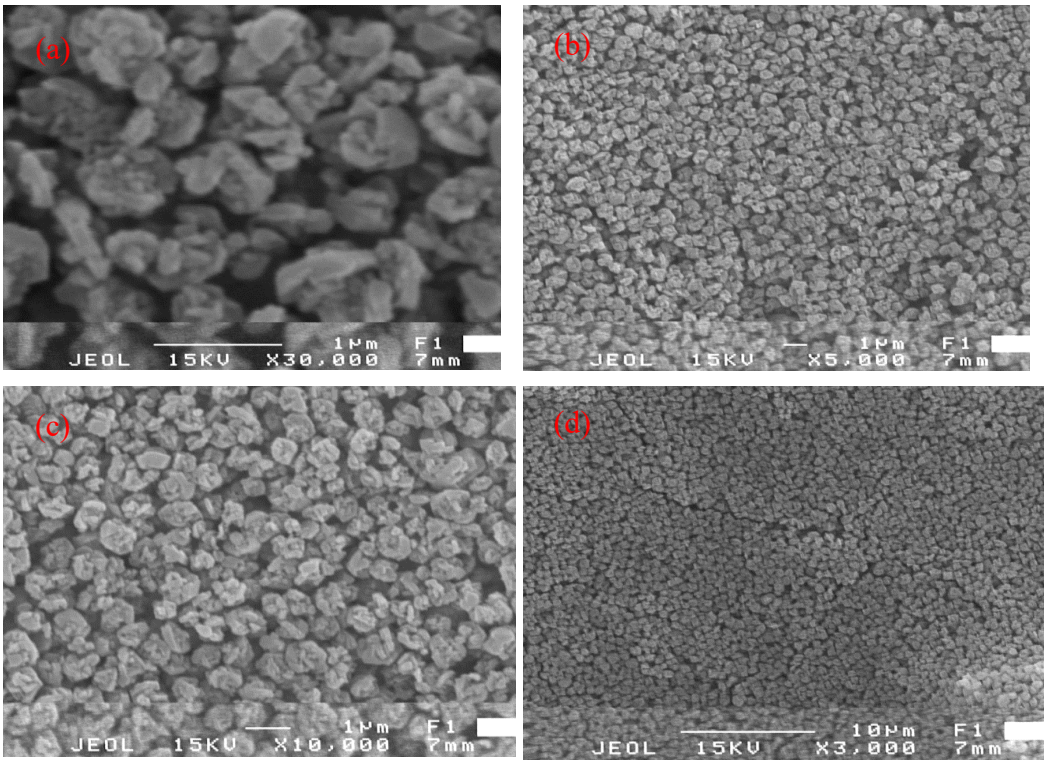

Figure 5: SEM images of Z-RHA (a,b) and TMZ-RHA (c,d)

Conclusions

Rice husk ash, an abundant solid waste in Vietnam, can be converted to a mesoporous zeolite which is one of the highly promising materials due to its micro/mesopore structure. The mesoporous zeolite was successfully prepared by the top-down method in which common acid and base were used as leaching agents. The mesoporous zeolite was also obtained by bottom-up approach with a addition of cationic surfactant during the hydrothermal step. The obtained zeolite material possessed mesopores (3-6 nm) while the zeolite structure was still retained. Thanks to the SiO_2 extraction method from rice husk ash to form an intermediate product of FAU zeolite. Comparing to the traditional zeolite, the mesoporous zeolite had a significantly higher mesopore surface area as well as higher pore volume. Further research work on the application of the mesoporous zeolite will be conducted in the future to utilize the special properties of this low-cost material in practice.

Acknowledgments

The authors would like to thank the Department of Science and Technology- Ho Chi Minh City (No.39/2019/HĐ-QKHCN) for financially supporting this research.

References

1. http://www.ricehuskash.com, assess on 11/07/2020.
2. Worrell E, Price L, Martin N, Hendriks C, Meida LO, Ann Rev Energy Environ: Carbon dioxide emissions from the global cement industry 1, (2001) 29-303. https://doi.org/10.1146/annurev.energy.26.1.303
3. VietnamBiz, 2019 rice market report, [Online]. Available https://vietnambiz.vn/, assess on 11/07/2020.
4. Faisal I. Khan, Aloke Kr. Ghoshal, "Review Removal of Volatile Organic Compounds from polluted air", Journal of Loss Prevention in the Process Industries 13, (2000) 527–545. https://doi.org/10.1016/S0950-4230(00)00007-3
5. Sanjaya D. Perera, Ruperto G. Mariano, Khiem Vu, Nijem Nour, Oliver Seitz, Yves Chabal and Kenneth J. Balkus, Jr. Hydrothermal Synthesis of Graphene-TiO_2 Nanotube Composites with Enhanced Photocatalytic Activity", in ACS Catalyst, (2012). https://doi.org/10.1021/cs200621c
6. Huitong Wu et al, Facile & Hydrothermal Synthesis Of TiO_2 Nanospindles-Reduced Graphene Oxide Composite With A Enhanced Photocatalytic Activity., in Journal of alloys and compounds, (2014). https://doi.org/10.1016/j.jallcom.2014.10.153
7. Bakar, Ayu Haslija Abu, and Chong Jia Ni Carey. Extraction of Silica from Rice Straw Using Alkaline Hydrolysis Pretreatment. In IOP Conference Series: Materials Science and Engineering, 778, no. 1, (2020) 012158. https//doi.org/10.1088/1757-899X/778/1/012158
8. Amin Kalantarifard, Amin Ghavaminejad and Go Su Yang, High CO_2 adsorption on improved ZSM-5 zeolite porous structure modified with ethylenediamine and desorption characteristics with microwave, (2015). https//doi.org/10.14912/jsmcwm.26.0_574
9. James C, Fisher II, Tanthana J, Chuang S, Oxide-supported tetraethylenepentamine for CO_2 capture, Environ Prog Sustain Energy, (2009) 589–598,
10. T. T. Xu, C. F Xue, Z. L. Zhang and X. G. Hao, Prog. Chem, 26, (2014) 1924–1929. https://doi.org/10.7536/PC140809
11. D. Bradshaw, S. El-Hankari and L. Lupica-Spagnolo, Chem. Soc. Re, 43, (2014) 5431–5443. https://doi.org/10.1039/C4CS00127C
12. Princiotta, F, Global Climate Change, The Technology Challenge, (2011). https://doi.org/10.1007/978-90-481-3153-2
13. Álvarez, A., Bansode, A., Urakawa, A., Bavykina, A. V., Wezendonk, T. A., Makkee, M., et al., Challenges in the greener production of formates/formic acid, methanol, and DME by heterogeneously catalyzed CO_2 hydrogenation processes, 117, (2017) 9804–9838,. https://doi.org/10.1021/acs.chemrev.6b00816
14. Mustapa, S. I., Leong Yow, P., and Hashim, A. H, Issues and challenges of renewable energy development: a Malaysian experience, in Proceedings of the International Conference on Energy and Sustainable Development: Issues and Strategies, (2010) 1–6. . https://doi.org/10.1109/ESD.2010.5598779
15. Zahida Rafig, Rabia Nazir, Muhammad Naeem Khan and Murtaza Saleem, Utilization of magnesium and zinc oxide nano-adsorbents as potential materials for treatment of copper electroplating industry wastewater, Journal of Environmental Chemical Engineering, (2014). https://doi.org/10.1016/j.jece.2013.11.004
16. García-Martínez, J., Johnson, M., Valla, J., Li, K., & Ying, J. Y., Mesostructured zeolite Y—high hydrothermal stability and superior FCC catalytic performance. Catalysis Science & Technology, 2(5), (2012) 987-994. https://doi.org/10.1039/C2CY00309K